Applied Physics Letters

Quantum transport in high-quality shallow InSb quantum wells

Cite as: Appl. Phys. Lett. **115**, 012101 (2019); https://doi.org/10.1063/1.5098294
Submitted: 01 April 2019 . Accepted: 17 June 2019 . Published Online: 01 July 2019

Zijin Lei, Christian A. Lehner, Erik Cheah, Matija Karalic, Christopher Mittag, Luca Alt, Jan Scharnetzky, Werner Wegscheider, Thomas Ihn, and Klaus Ensslin

Applied Physics Letters ARTICLE scitation.org/journal/apl

Quantum transport in high-quality shallow InSb quantum wells

Cite as: Appl. Phys. Lett. **115**, 012101 (2019); doi: 10.1063/1.5098294
Submitted: 1 April 2019 · Accepted: 17 June 2019 ·
Published Online: 1 July 2019

Zijin Lei,[a),b)] Christian A. Lehner,[a)] Erik Cheah, Matija Karalic, Christopher Mittag, Luca Alt, Jan Scharnetzky, Werner Wegscheider, Thomas Ihn, and Klaus Ensslin

AFFILIATIONS

Solid State Physics Laboratory, Department of Physics, ETH Zurich, 8093 Zurich, Switzerland

[a)]**Contributions:** Z. Lei and C. A. Lehner contributed equally to this work.
[b)]**Electronic mail:** zilei@phys.ethz.ch

ABSTRACT

InSb is one of the promising candidates to realize a topological state through proximity induced superconductivity in a material with strong spin–orbit interactions. In two-dimensional systems, thin barriers are needed to allow strong coupling between superconductors and semiconductors. However, it is still challenging to obtain a high-quality InSb two-dimensional electron gas in quantum wells close to the surface. Here, we report on a molecular beam epitaxy grown heterostructure of InSb quantum wells with substrate-side Si-doping and ultrathin InAlSb (5 nm, 25 nm, and 50 nm) barriers to the surface. We demonstrate that the carrier densities in these quantum wells are gate-tunable and electron mobilities up to 350 000 $cm^2(V\ s)^{-1}$ are obtained from magnetotransport measurements. Furthermore, from temperature-dependent magnetoresistance measurements, we obtain an effective mass of 0.02 m_0 and find Zeeman splitting compatible with the expected band edge g-factor.

InSb elicits special interest in electronic,[1,2] electro-optical,[3] and spintronic[4] applications due to its unique and extreme properties compared to other binary III-V compound semiconductors. Apart from the small bandgap and electron effective mass, InSb is considered a candidate for the fabrication of topological quantum devices owing to its strong Rashba spin–orbit interaction (SOI)[5–7] and its intrinsic giant band edge g-factor of $|g| \sim 51$.[8,9] As proposed by Oreg *et al.*,[10] a topological superconducting phase can be induced in a one-dimensional semiconductor with strong Rashba SOI in a Zeeman field by the coupling to an s-wave superconductor. Reports in this regard have been published for InAs[11] and InSb[12] nanowire-based Majorana devices. In contrast to nanowires, two-dimensional electron gas (2DEG) systems are far more versatile for topological applications. Various types of scalable superconductor-semiconductor hybrid devices have been proposed,[13–15] and experimental research in Al-InAs heterostructures[16–18] has hence followed. However, despite the superior intrinsic material properties, the progress of InSb 2DEGs is still hampered. Recently, there has been development in free-standing InSb nanostructures and their transport measurements, such as nanosails[19] and nanosheets.[20–22] These layered InSb structures have advantages to achieve direct metal/superconductor contacts on them. Nevertheless, the research on InSb quantum wells (QWs) is still lacking due to the difficulties with heterostructure growth although QWs have significant potential leading to high-quality devices.[23,24] In QW systems, a thin barrier is required to induce superconductivity in the 2DEG through the proximity effect. However, the closeness of the 2DEG to the surface can limit the mobility of the carriers as a consequence. In this work, we present a quantum transport experiment, where the InSb 2DEG is close to the sample surface. Our magnetotransport measurements show that the 2DEGs still preserve a high mobility, even for the case of a QW with a barrier to the surface of only 5 nm. We also investigate other unique characteristics of InSb, such as the light electron effective mass m^* and the large band edge g-factor.

We report the fabrication and characterization of three InSb QW samples doped on the substrate side, which are grown on (100) GaAs substrates by molecular beam epitaxy (MBE). Two schematic layer sequences are shown in Figs. 1(a) and 1(b). The growth details introduced in Ref. 25 are only briefly outlined here. To overcome the lattice mismatch between GaAs and InSb, an interfacial misfit GaSb buffer and an interlayer InAlSb buffer are employed. The total thickness of this buffer system amounts to roughly 3 μm. The 21 nm-thin InSb QWs are then surrounded by $In_{0.9}Al_{0.1}Sb$ confinement barriers, while n-type carriers are introduced to the active region by a Si δ-doping layer incorporated 30 nm below the QW in the barrier on the substrate

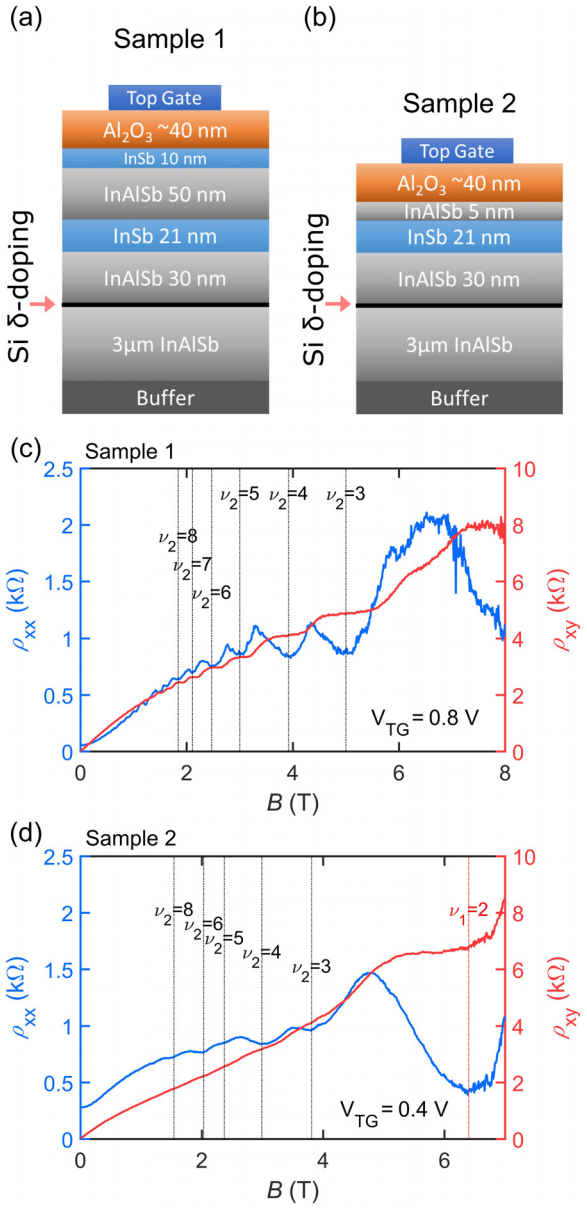

FIG. 1. (a) Layer structure of sample 1. (b) Layer structure of sample 2. The *B*-dependences of ρ_{xx} (blue) and ρ_{xy} (red) of sample 1 and sample 2 are shown in (c) and (d), respectively. The filling factor of the electrons in the doping layer, ν_1, and the filling factor of the electrons in the QW, ν_2, are determined from the SdH data.

side. On top of the QW, the $In_{0.9}Al_{0.1}Sb$ layer thicknesses for samples 1 and 2 are 50 nm and 5 nm, respectively. Sample 1 is the only sample entailing a 10 nm InSb capping layer, while for samples 2 and 3 (25 nm thick upper barrier), the structure ends with $In_{0.9}Al_{0.1}Sb$ [see Fig. 1(b)]. We adopt the asymmetric bottom-doping scheme to avoid screening of the top gate electric field by the doping layer. A self-consistent band structure simulation of these 3 samples is introduced in the supplementary material.

Using wet chemical etching, standard Hall bar structures are defined with an etch depth higher than 120 nm, which is thus deeper than the Si-doping layer. Hall bar samples 1 and 2 have lateral dimensions of 50×25 μm^2 (contact separation×width), while sample 3 is 10×4 μm^2 in size. Layers of Ge/Ni/Au evaporated on the contact areas of the samples after an Ar sputtering process provide Ohmic contacts to the 2DEG without the necessity of annealing.[26] The samples are coated with a 40 nm-thick aluminum oxide (ALO) dielectric layer using atomic layer deposition at a temperature of 150 °C. Finally, Ti/Au top gates covering the Hall bars are evaporated using electron beam evaporation. As a comparison, van der Pauw geometry samples without chemical etching and ALO are fabricated from the same wafers of the Hall bar samples. Their magnetotransport measurement is introduced in the supplementary material.

Magnetotransport characterization is performed using standard low frequency (12 Hz) lock-in techniques at a temperature of 1.3 K. Figures 1(c) and 1(d) show the dependence of the longitudinal and transverse resistivities ρ_{xx} and ρ_{xy} of samples 1 and 2 in a magnetic field B applied normal to the QW plane, where the top gate voltages V_{TG} are 0.8 V and 0.4 V, respectively. Shubnikov-de Haas oscillations in ρ_{xx} and plateaus in ρ_{xy} can be seen. In addition, the positive magnetoresistance and the nonlinear Hall resistance found in both samples at fields below about 4 T imply the existence of parallel conducting channels with distinct mobilities. Thus, the plateaus in ρ_{xy} are not quantized at the expected values of the single-subband quantum Hall effect. The origin of the parallel channels is discussed below.

In the following, we describe the properties of sample 2 in detail, as it comprises the thinnest barrier. It is, therefore, most interesting with regard to a superconducting proximity effect induced by a superconducting contact. The details of samples 1 and 3 are given in the supplementary material. Figures 2(a) and 2(b) show ρ_{xx} and ρ_{xy} for sample 2 as a function of the top gate voltage V_{TG} and the magnetic field B, respectively. Figure 2(a) shows two Landau fan diagrams, the first of which appears at low V_{TG} and is marked with blue dashed lines, while the second Landau fan diagram at high V_{TG} is marked with white dashed lines. The double-fan structure confirms the presence of two parallel conducting channels in the heterostructure. We extract their carrier densities n_1 and n_2 from the $1/B$ periodicity of the SdH oscillations. As shown in Fig. 3(a), at lower V_{TG}, only the first channel is populated and the density n_1 increases linearly with increasing V_{TG}. When $V_{TG} > -0.1$ V, the increase in n_1 saturates, while the second channel gets populated and n_2 increases linearly instead. The gate capacitances of the first and second channels are estimated to be $C_1 = 0.7$ mF/m^2 and $C_2 = 1.02$ mF/m^2, respectively. We attribute n_1 to carriers in the Si-doping layer and n_2 to carriers in the QW. The calculated capacitances are within a factor of two of what is expected by considering the layer thicknesses and dielectric constants. The saturation of n_1 is due to screening of the gate electric field by the electrons populating the QW.

A two-band Drude model allows us to estimate the mobilities μ_1 and μ_2 of Si and the QW layer electrons. Using n_1 and n_2 obtained from the SdH oscillations, only the two mobilities remain as fitting parameters. As shown in Fig. 3(b), the mobility μ_2 increases with the increase in V_{TG}. The inset of Fig. 3(b) shows data (circles) and fitted curves (lines) of the low field ρ_{xx} and ρ_{xy} of sample 2 at a gate voltage of $V_{TG} = 0.4$ V in a small magnetic field range. With $n_1 = 3 \times 10^{15}$ m^{-2} and $n_2 = 3 \times 10^{15}$ m^{-2}, we find that mobilities are $\mu_1 = 7500$ cm^2 (V s)$^{-1}$

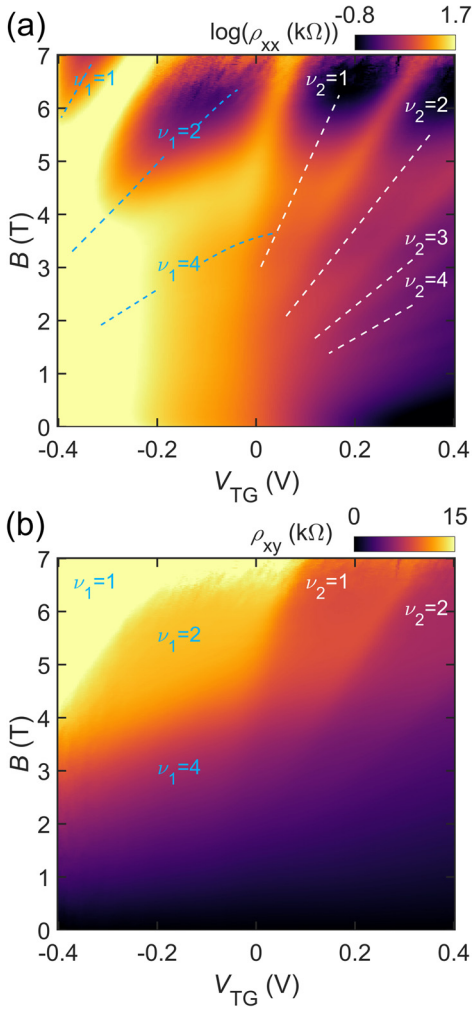

FIG. 2. The detailed transport characterization of sample 2 at 1.3 K with ρ_{xx} (a) and ρ_{xy} (b) as functions of V_{TG} and B. The Landau fan diagrams and filling factors of the electrons in the doping layer and QW layer are labeled with blue and white dashed lines, respectively.

and $\mu_2 = 67\,000\ \mathrm{cm^2(V\,s)^{-1}}$, respectively. Phenomenologically, samples 1 and 3 behave similarly, and their densities and mobilities are listed in Table I. Specifically, compared to previous related publications,[5,9,23,24,27–30] sample 1 still holds similar or higher mobility of the 2DEG with a comparable or thinner barrier thickness.

From temperature-dependent SdH oscillations, it is found that the effective mass of the electrons in the InSb QWs can be determined. Figure 4(a) shows the corresponding measurements for sample 2 with $n_2 = 3.8 \times 10^{15}\ \mathrm{m^{-2}}$ determined from the $1/B$-periodicity. The oscillations of the resistivity $\Delta\rho_{xx}$ are obtained by subtracting the smooth background of the magnetoresistance $\bar{\rho}_{xx}$.[31] Figure 4(b) shows fits of the Dingle factor[32] to $\ln(\rho_{xx}/\bar{\rho}_{xx})$. The obtained effective mass is $m^* \approx 0.019\ m_0$, where m_0 is the electron mass in vacuum. Using the same method, we find that the effective mass is density-independent within the range between $1.8 \times 10^{15}\ \mathrm{m^{-2}}$ and $3.8 \times 10^{15}\ \mathrm{m^{-2}}$. This result is consistent with the recent work of Ke *et al.*[24]

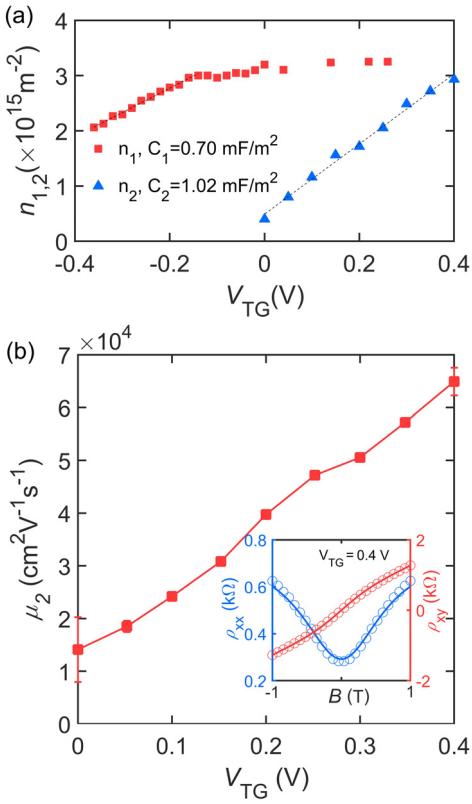

FIG. 3. Analysis of the data shown in Fig. 2. (a) Carrier densities of the two conductive channels vs V_{TG}. (b) The mobility μ_2 extracted from the two-band model vs V_{TG}. Inset: the data (circles) and fitting (lines) of ρ_{xx} (red) and ρ_{xy} (blue) vs B when $V_{TG} = 0.4$ V.

The spin-splitting of Landau levels is observed at a magnetic field of 2 T, as shown in the inset of Fig. 4(a). With increasing B, the integer filling factor sequence changes from even to even and odd numbers. The magnetic field value beyond which the spin-splitting is resolved in the experiment is consistent with the band edge g-factor values determined in similar InSb QWs[25] and the works in InSb nanoconstrictions.[8,24,33,34] A very rough estimate of the band edge g-factor for our device is found in the supplementary material.

In summary, we have presented an InSb QW heterostructure with inverted doping and ultrathin InAlSb barriers to the sample surface. Using a standard Hall bar geometry, we performed magneto-transport measurements and found that the InSb QWs still show tunable densities and high mobilities, despite the small barrier thickness. The parallel conducting channel induced by the Si doping found in

TABLE I. Summary of carrier densities, mobilities, and effective masses of all the three samples in this work.

Properties	Sample 1	Sample 2	Sample 3
Upper barrier thickness	50 nm	5 nm	25 nm
$\mu_{2(max)}$ [cm^2 (V s)$^{-1}$]	350 000	67 000	160 000
n_2($\times 10^{15}$ m^{-2})	0–3.5	0–3	0–3
m^*	0.020 m_0	0.019 ± 0.02 m_0	…

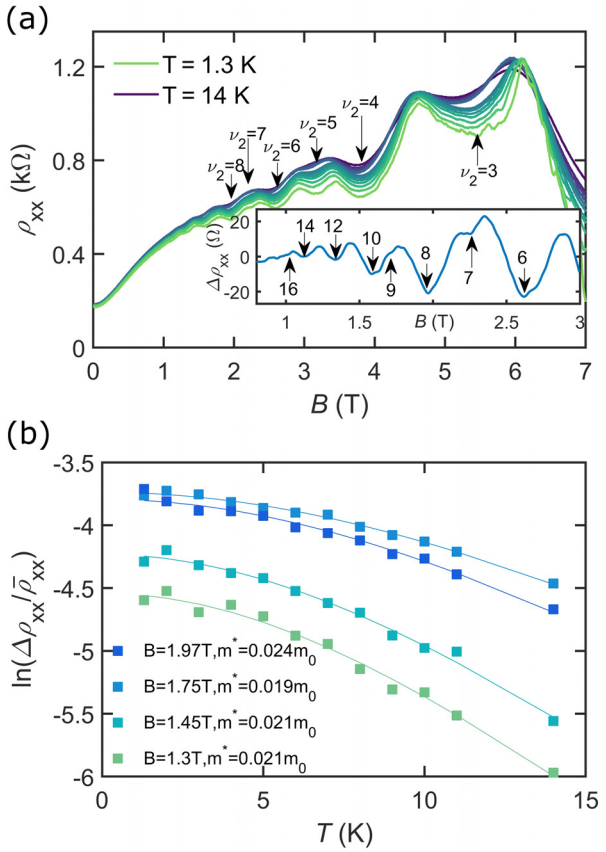

FIG. 4. Effective mass measurement and the Zeeman splitting of sample 2. (a) Temperature-dependence of SdH oscillations with $n_2 = 3.8 \times 10^{15}$ m^{-2}. Inset: $\Delta\rho_{xx}$ in a small magnetic field measured at 1.3 K. The Zeeman splitting occurs at around $\nu_2 = 9$. (b) Dingle factor fitting with different B values. The squares are data, and the lines are fitted curves.

the investigated samples can be eliminated by reducing the doping concentration in future devices. We determined the effective in-plane mass of electrons in the InSb QWs to be 0.019 m_0 and estimated a large band edge g-factor close to the intrinsic bulk value. We anticipate that this work paves the way for realizing in-plane InSb devices with a superconducting top gate in the future, where Andreev reflection and 2D Majorana physics may be investigated.

See the supplementary material for the band edge g-factor estimation, the self-consistent band structure simulation, and the magnetotransport measurements of sample 1, sample 3, and the van der Pauw geometry samples.

This work was supported by the Swiss National Science Foundation through the National Center of Competence in Research (NCCR) Quantum Science and Technology.

REFERENCES

[1]T. Ashley, A. Dean, C. Elliott, G. Pryce, A. Johnson, and H. Willis, "Uncooled high-speed InSb field-effect transistors," Appl. Phys. Lett. **66**, 481–483 (1995).
[2]J. Orr, P. Buckle, M. Fearn, C. Storey, L. Buckle, and T. Ashley, "A surface-gated InSb quantum well single electron transistor," New J. Phys. **9**, 261 (2007).
[3]H. Chen, J. Heremans, J. Peters, A. Govorov, N. Goel, S. Chung, and M. Santos, "Spin-polarized reflection in a two-dimensional electron system," Appl. Phys. Lett. **86**, 032113 (2005).
[4]I. Žutić, J. Fabian, and S. D. Sarma, "Spintronics: Fundamentals and applications," Rev. Mod. Phys. **76**, 323 (2004).
[5]M. Leontiadou, K. Litvinenko, A. Gilbertson, C. Pidgeon, W. Branford, L. Cohen, M. Fearn, T. Ashley, M. Emeny, B. Murdin *et al.*, "Experimental determination of the Rashba coefficient in InSb/InAlSb quantum wells at zero magnetic field and elevated temperatures," J. Phys.: Condens. Matter **23**, 035801 (2011).
[6]R. Kallaher, J. Heremans, N. Goel, S. Chung, and M. Santos, "Spin-orbit interaction determined by antilocalization in an InSb quantum well," Phys. Rev. B **81**, 075303 (2010).
[7]G. Khodaparast, R. Doezema, S. Chung, K. Goldammer, and M. Santos, "Spectroscopy of Rashba spin splitting in InSb quantum wells," Phys. Rev. B **70**, 155322 (2004).
[8]F. Qu, J. van Veen, F. K. de Vries, A. J. Beukman, M. Wimmer, W. Yi, A. A. Kiselev, B.-M. Nguyen, M. Sokolich, M. J. Manfra *et al.*, "Quantized conductance and large g-factor anisotropy in InSb quantum point contacts," Nano Lett. **16**, 7509–7513 (2016).
[9]A. Gilbertson, W. Branford, M. Fearn, L. Buckle, P. D. Buckle, T. Ashley, and L. Cohen, "Zero-field spin splitting and spin-dependent broadening in high-mobility InSb/$In_{1-x}Al_xSb$ asymmetric quantum well heterostructures," Phys. Rev. B **79**, 235333 (2009).
[10]Y. Oreg, G. Refael, and F. von Oppen, "Helical liquids and Majorana bound states in quantum wires," Phys. Rev. Lett. **105**, 177002 (2010).
[11]M. Deng, S. Vaitiekėnas, E. B. Hansen, J. Danon, M. Leijnse, K. Flensberg, J. Nygård, P. Krogstrup, and C. M. Marcus, "Majorana bound state in a coupled quantum-dot hybrid-nanowire system," Science **354**, 1557–1562 (2016).
[12]H. Zhang, C.-X. Liu, S. Gazibegovic, D. Xu, J. A. Logan, G. Wang, N. Van Loo, J. D. Bommer, M. W. De Moor, D. Car *et al.*, "Quantized Majorana conductance," Nature **556**, 74 (2018).
[13]R. P. Riwar, M. Houzet, J. S. Meyer, and Y. V. Nazarov, "Multi-terminal Josephson junctions as topological matter," Nat. Commun. **7**, 11167 (2016).
[14]A. Stern and E. Berg, "Fractional Josephson vortices and braiding of Majorana zero modes in planar superconductor-semiconductor heterostructures," Phys. Rev. Lett. **122**, 107701 (2019).
[15]Y. Peng, F. Pientka, E. Berg, Y. Oreg, and F. von Oppen, "Signatures of topological Josephson junctions," Phys. Rev. B **94**, 085409 (2016).
[16]H. J. Suominen, M. Kjaergaard, A. R. Hamilton, J. Shabani, C. J. Palmstrøm, C. M. Marcus, and F. Nichele, "Zero-energy modes from coalescing Andreev states in a two-dimensional semiconductor-superconductor hybrid platform," Phys. Rev. Lett. **119**, 176805 (2017).
[17]A. Fornieri, A. M. Whiticar, F. Setiawan, E. Portolés, A. C. Drachmann, A. Keselman, S. Gronin, C. Thomas, T. Wang, R. Kallaher *et al.*, "Evidence of topological superconductivity in planar Josephson junctions," Nature **569**, 1 (2019).
[18]A. Whiticar, A. Fornieri, E. O'Farrell, A. Drachmann, T. Wang, C. Thomas, S. Gronin, R. Kallaher, G. Gardner, M. Manfra *et al.*, "Interferometry and coherent single-electron transport through hybrid superconductor-semiconductor Coulomb islands," preprint arXiv:1902.07085 (2019).
[19]M. de la Mata, R. Leturcq, S. R. Plissard, C. Rolland, C. Magen, J. Arbiol, and P. Caroff, "Twin-induced InSb nanosails: A convenient high mobility quantum system," Nano Lett. **16**, 825–833 (2016).
[20]D. Pan, D. Fan, N. Kang, J. Zhi, X. Yu, H. Xu, and J. Zhao, "Free-standing two-dimensional single-crystalline InSb nanosheets," Nano Lett. **16**, 834–841 (2016).
[21]N. Kang, D. Fan, J. Zhi, D. Pan, S. Li, C. Wang, J. Guo, J. Zhao, and H. Xu, "Two-dimensional quantum transport in free-standing InSb nanosheets," Nano Lett. **19**, 561–569 (2019).
[22]J. Xue, Y. Chen, D. Pan, J.-Y. Wang, J. Zhao, S. Huang, and H. Xu, "Gate defined quantum dot realized in a single crystalline InSb nanosheet," Appl. Phys. Lett. **114**, 023108 (2019).
[23]W. Yi, A. A. Kiselev, J. Thorp, R. Noah, B.-M. Nguyen, S. Bui, R. D. Rajavel, T. Hussain, M. F. Gyure, P. Kratz *et al.*, "Gate-tunable high mobility remote-

doped InSb/$In_{1-x}Al_xSb$ quantum well heterostructures," Appl. Phys. Lett. **106**, 142103 (2015).
[24]C. T. Ke, C. M. Moehle, F. K. de Vries, C. Thomas, S. Metti, C. R. Guinn, R. Kallaher, M. Lodari, G. Scappucci, T. Wang *et al.*, "Ballistic superconductivity and tunable π-junctions in InSb quantum wells," preprint arXiv:1902.10742 (2019).
[25]C. A. Lehner, T. Tschirky, T. Ihn, W. Dietsche, J. Keller, S. Fält, and W. Wegscheider, "Limiting scattering processes in high-mobility InSb quantum wells grown on GaSb buffer systems," Phys. Rev. Mater. **2**, 054601 (2018).
[26]N. Goel, J. Graham, J. Keay, K. Suzuki, S. Miyashita, M. Santos, and Y. Hirayama, "Ballistic transport in InSb mesoscopic structures," Physica E **26**, 455–459 (2005).
[27]O. Pooley, A. Gilbertson, P. Buckle, R. Hall, M. Emeny, M. Fearn, M. Halsall, L. Cohen, and T. Ashley, "Quantum well mobility and the effect of gate dielectrics in remote doped InSb/$Al_xIn_{1-x}Sb$ heterostructures," Semicond. Sci. Technol. **25**, 125005 (2010).
[28]F. Gouider, Y. B. Vasilyev, M. Bugár, J. Könemann, P. Buckle, and G. Nachtwei, "Terahertz photoresponse of AlInSb/InSb/AlInSb quantum well structures," Phys. Rev. B **81**, 155304 (2010).
[29]M. Uddin, H. Liu, K. Yang, K. Nagase, T. Mishima, M. Santos, and Y. Hirayama, "Characterization of InSb quantum wells with atomic layer deposited gate dielectrics," Appl. Phys. Lett. **101**, 233503 (2012).
[30]J. Mlack, K. Wickramasinghe, T. Mishima, M. Santos, and C. Marcus, "In-plane magnetoconductance mapping of InSb quantum wells," preprint arXiv:1902.07570 (2019).
[31]B. Habib, M. Shayegan, and R. Winkler, "Spin-orbit interaction and transport in GaAs two-dimensional holes," Semicond. Sci. Technol. **23**, 064002 (2009).
[32]T. Ihn, *Semiconductor Nanostructures: Quantum States and Electronic Transport* (Oxford University Press, 2010).
[33]H. A. Nilsson, P. Caroff, C. Thelander, M. Larsson, J. B. Wagner, L.-E. Wernersson, L. Samuelson, and H. Xu, "Giant, level-dependent g factors in InSb nanowire quantum dots," Nano Lett. **9**, 3151–3156 (2009).
[34]H. Nilsson, O. Karlström, M. Larsson, P. Caroff, J. N. Pedersen, L. Samuelson, A. Wacker, L.-E. Wernersson, and H. Xu, "Correlation-induced conductance suppression at level degeneracy in a quantum dot," Phys. Rev. Lett. **104**, 186804 (2010).